



The effects of additive on photovoltaic performance of $\text{Cu}_2\text{ZnSnS}_4$ promising solar absorbers

Samed Çetinkaya *¹ 

¹Mersin University, Department of Medical Services and Techniques, Mersin, Türkiye, samedcetinkaya@mersin.edu.tr

Cite this study: Çetinkaya, S. (2023). The effects of additive on photovoltaic performance of $\text{Cu}_2\text{ZnSnS}_4$ promising solar absorbers. *Advanced Engineering Science*, 3, 178-187

Keywords

Ethyl cellulose
CZTS
Solar cell
Additives
IPCE efficiency

Research Article

Received:25.09.2023
Revised: 19.10.2023
Accepted:24.10.2023
Published:31.10.2023



Abstract

In this study, the effect of ethyl cellulose as an additive on the structural, morphological and electrical properties of CZTS thin films was investigated. It was observed that the morphology and characteristic properties improved with the increase of the ethyl cellulose additive ratio. Despite the contribution, no binary and/or ternary phases formed and the formation of CZTS thin films determined by Raman spectroscopy. It was observed that uniformly distributed, continuous and dense granules with a thickness of approximately 1-2 μm were formed, when the surface morphology ratio of the ethyl cellulose-0.9% was submitted. In addition, it was determined from the obtained results that these surface properties contributed positively to the IPCE efficiency measurements. Accordingly, the highest IPCE efficiency was calculated as 10.63%. Finally, the estimation of the optical absorption measurement results is in between 1.37 and 1.60 eV interpreted to be in agreement with the literature values.

1. Introduction

Cu-Zn-Sn-S compound is an emerging and very promising for solar absorber photovoltaic (PV) materials due to it contains earth-abundant and low toxicity elements [1]. This situation expected to contribute in the future to reduce fabrication costs. Among the new generation/alternative absorber materials, $\text{Cu}_2\text{ZnSnS}_4$ (CZTS) compound, is a good candidate for an absorber layer in solar cell applications. Although the calculated theoretical yield for quaternary compounds as 32.2% [2], the highest achievable laboratory yield for the CZTS compound is 12.6% by Todorov and co-workers [3].

CZTS compound is a p-type quaternary semiconductor with a kesterite crystal structure. Each element of the CZTS compound is abundant in the Earth's crust (Cu: 50 ppm, Zn: 75 ppm, Sn: 2.2 ppm, S: 350 ppm) and has a lower toxic effect [4-6]. The CZTS compound has a direct band gap of 1.4-1.5 eV and a high absorption coefficient of 104 cm^{-1} . In addition, this compound does not contain toxic and expensive elements such as Selenium (Se) or Cadmium (Cd) used in current commercial solar cells, so on the contrary, it includes the elements of environmentally friendly [7]. The photovoltaic effect on a CZTS-based heterojunction diode was for the first time reported by Ito and Nakazawa in 1988 [4].

In the literature, there are various deposition techniques to obtain CZTS thin films such as physical vapor deposition (PVD) [8-18], sol-gel spin coating [19-29], electrochemical deposition (ECD) [30-33], and SILAR methods [34-38]. Among of them, liquid phase storage techniques are relatively cheaper and are suitable for using various types of substrates with larger surfaces. In addition, the quality of the films obtained by these methods is comparable to those obtained by physical methods [39].

Researchers have tried in order to increase the efficiency values of commercial solar cells available in the literature [40]. One of the most effective of these is to use surfactant/additives doping. In general, doping is used to control growth mechanism, particle size, crystal structure, conductivity and surface morphology in solution growth methods. The efficiency of thin-film based solar cells is directly related with the surface morphology, and generally, the best way to increase this efficiency is to dope the films using appropriate additives. It has been reported that ethyl cellulose (ETS) increases the ionic conductivity and can reduce the cracks formed on the film surface, thus increasing the battery efficiency [41-44].

To the best of my knowledge, there are no reports on investigating the effect of ETS on CZTS thin-film based solar cells, yet. In this study, the effect of ethyl cellulose concentration on the quantum yield, morphology, optical and structural properties of CZTS thin films containing inexpensive and environmentally friendly elements was investigated for the first time in the literature.

2. Material and Method

CZTS thin films were deposited on pre-cleaned on Molybdenum coated soda lime glass (MSLG) substrates by spin coating method. The substrates were ultrasonically cleaned in turn with detergent, nitric acid (1:4), acetone and ethanol for 10 min., as our previous study [45]. The solution containing basically copper (II) acetate monohydrate (0.3 M, 98+%), zinc (II) acetate dihydrate (0.3 M, 99.99%), tin (II) chloride (0.3 M, 98%) and thiourea (1.2 M, 99.0+% from Sigma Aldrich) into 2-methoxyethanol (20 ml, 99.8% from Sigma Aldrich). 2.5 ml of diethanolamine (DEA) were added slowly into the solution as a stabilizer while stirring. Then, the solution was stirred at 45 °C, 850 rpm for 1 h for dissolve the metal compounds completely. The final solution was poured into six beakers and added to each solution at 0.1 intervals between 0.8% and 1.3% with ethyl cellulose dissolved in 2-methoxyethanol (from Sigma Aldrich). The films were labelled within the text as S0: undoped CZTS and S1: (0.80%), S2: (0.90%), S3: (1.00%); S4: (1.10%); S5: (1.20%) and S6: (1.30%) ETS-doped CZTS, respectively. To deposit the CZTS films, the precursor solutions were spin-coated on to the substrates at 3000 rpm for 30 s followed by solvent-drying at 175 °C for 10 min on a hot plate. The fabrication processes were repeated 10 times to obtain the desired thickness of the films. Finally, the samples were subjected to an annealing process for 2 h at 500 °C in a quartz tube containing 10 grams of elemental sulfur. Before the heat-treatment, the furnace was evacuated to 5×10^{-4} mbar. The heating rate was 5 °C/min. After the heat-treatment, the samples were allowed to cool naturally to room temperature. The structural and morphological properties of the samples were examined by Raman spectroscopy (Confocal Raman spectrometer, Witec alpha 300 with 532 nm light source), scanning electron microscopy (FEI, Quanta FEG 250) methods, respectively.

In order to investigate the photovoltaic properties of pure CZTS and ethyl cellulose added thin films were applied to Incident photon-to-current efficiency (IPCE) measurements. To carry out the IPCE measurements, a monochromatic light source consisting of a 150 W Xe lamp and a monochromator were used to perform the IPCE measurements through an interfaced with computer by a Labview program.

3. Results and Discussion

3.1. Structural results

Raman spectroscopy is an efficient method to analyze the small changes as the vibrational signals are very sensitive to the local environment of the molecule, crystal structure, chemical bond, and so forth. ZnS, $\text{Cu}_2\text{X}_\text{S}$ and Cu_2SnS_3 have similar X-ray diffraction patterns to CZTS owing to their similar zinc blend-type structures (Figure 1) [46].

To prove the phase purity or to detect the presence of other possible secondary phases, Raman spectroscopy analyses results of ETS-doped CZTS thin films over the range 200–500 cm^{-1} was also made and the results were given in Figure 2. It can be seen from Figure 2, there is no linear change in the increase with the amount of additive. According to Figure 2, as one can see that the sharpest and most severe peak is in the sample named as S4.

The Raman peak of this sample tends to shift to the left (or lower wavenumber). In the literature, Raman spectroscopy analysis has shown variation of peaks to be a measure of phonon confinement [47,48] with shift in peak position related to grain size [48-52] and nature of defect on the grain boundaries [28,47]. A shift to lower wavenumbers is indicative of larger grain size [53]. From Figure 2, it can be seen that the peaks of the samples as named S2 and S4 tend to shift to the left. This situation can be interpreted because of the improvement of crystal quality and increase in grain size (Figure 3). In Raman analysis, red shift means that frequency of phonons interacting with the incident photon decreased. As seen in the Figure 2, vibrational peak at 333 cm^{-1} appeared for samples. According to this result, it can be said that the kesterite crystalline phase of CZTS is formed with any other binary and/or ternary secondary phases. The peaks are well agreement with the reference Raman spectra of CZTS and confirms the formation of the CZTS phase [54].

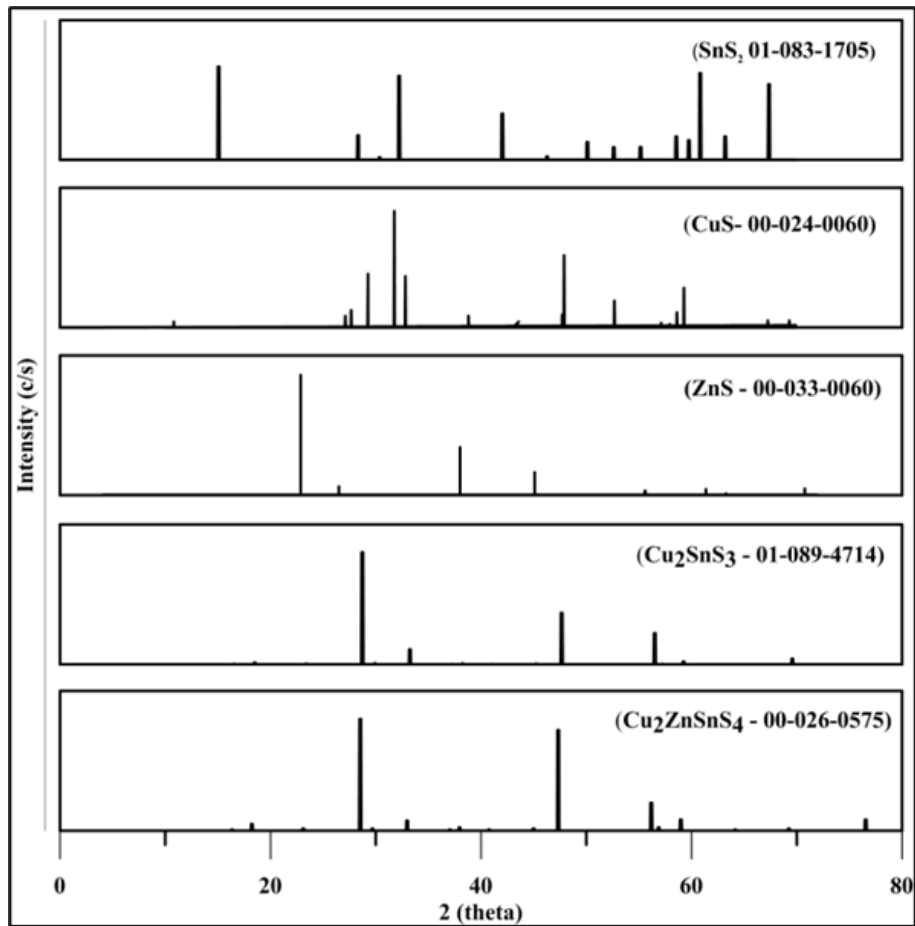


Figure 1. The X-Ray diffraction patterns of CZTS, CTS, CuS, ZnS and SnS2 along with reference pdf card numbers.

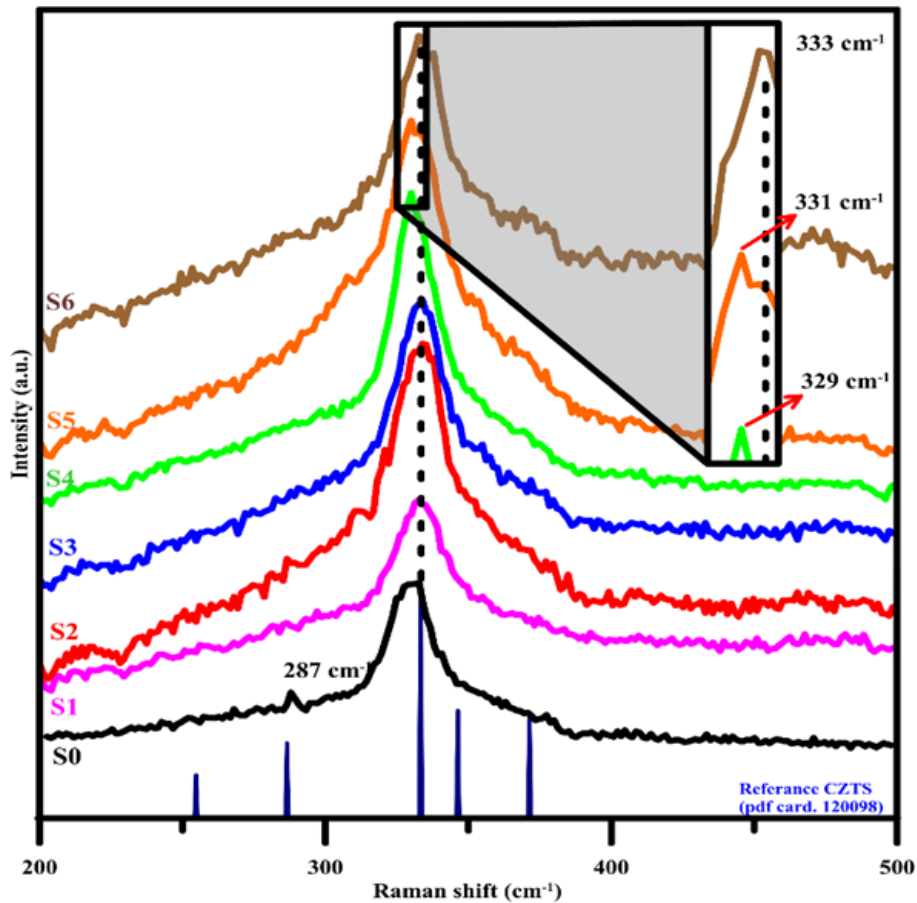


Figure 2. The Raman analysis results of pure and ETS-doped CZTS samples.

3.2. Surface morphology

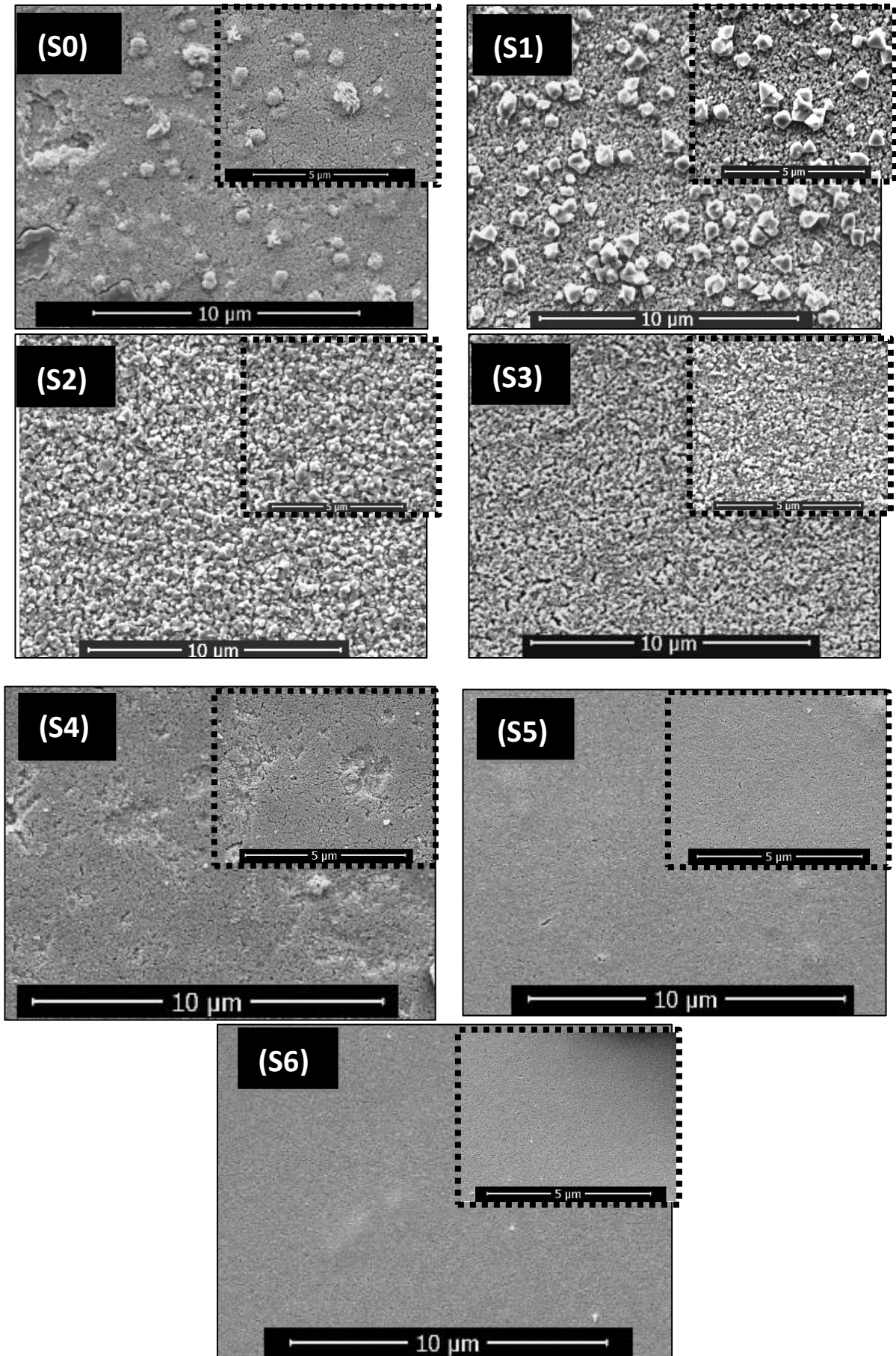


Figure 3. SEM micro-images of the S0-S6 thin films at various magnifications, respectively.

Figure 3 shows that the SEM images of the ETS-doped CZTS films deposited by using S0-S6 of ethyl cellulose, respectively. From Figure 3, it can be seen that the surface roughness of the films decreases with increasing ethyl cellulose content. The surface of the sample without ethyl cellulose (Figure 3) has cracks and has agglomeration like morphology than those of the samples with ethyl cellulose.

As seen in Figure 3, at the doping ratio from S1 to S3, there are a surface morphology consisting of large-grained structures with sizes ranging from approximately 1-2 μm , with cracks (Figure 3). It is also clear that, the sample prepared with S6 (Figure 3) is more continuous, homogeneously and without crack than others. As a first interpretation, regarding film morphology, increasing ethyl cellulose content in the sol-gel growth solution the smoother and continuous texture can be obtained. This enhancement may decrease the recombination and facilitate transport of photo-induced electrons. It has been reported in the literature that ETS contributes to electrical conductivity by reducing surface cracks and roughness in solar cell absorber layers [55, 56].

3.3. Incident photon-to-current efficiency (IPCE) characteristics

Incident Photon to Charge Carrier Efficiency (IPCE) – also referred to as Quantum efficiency (QE) – indicates the ratio of the number of photons from a monochromatic light source are converted to generated charge carriers. The IPCE yield curve gives information about recombination losses and absorption efficiency in the material.

Photovoltaic properties of ETS-doped CZTS thin films synthesized on Molybdenum coated SLG substrates via sol-gel spin coating technique were investigated using the IPCE measurements. The IPCE spectra show photocurrent response of the solar cells made of the ETS doped CZTS thin films. Figure 4, demonstrates the IPCE spectra for all samples.

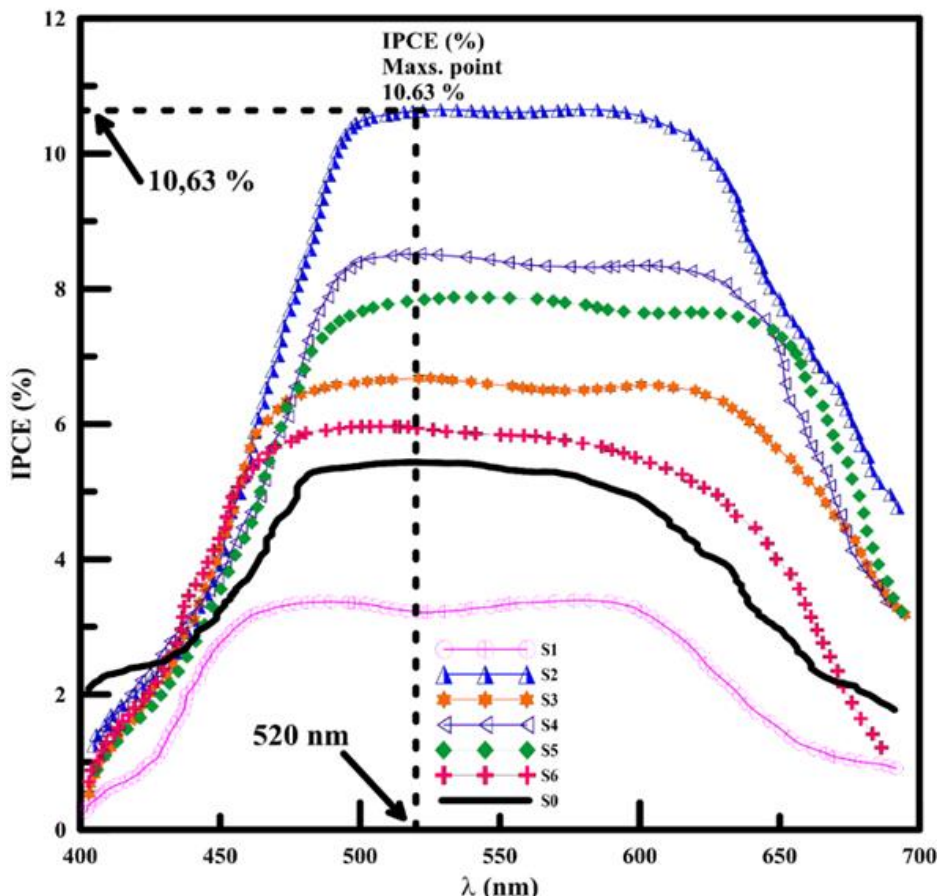


Figure 4. IPCE efficiency graph of the samples

From Figure 4, it was observed that the S2 labelled thin film had higher IPCE (%) efficiency value with 10.63% at 520 nm compared to the IPCE (%) value of pure CZTS thin film. Considerably increased grain sizes can be observed that the ratios of S2 (Figure 2(c, d)) which may affect the charge transport properties of the concluding S2. This result shows that the ETS additive plays an important role in the development of photovoltaic behavior of CZTS thin film. Because of, in high efficiency thin film solar cells, the surface of the absorber material consists of large granular structures without cracks, continuous and homogeneous distribution. In this way, less loss is experienced in electrical transmission.

From Figure 5, the peak of the IPCE of solar cells rise when the S2, implying that at this value the charge separation and collection becomes in efficient with large grain as before mentioned. It was also observed that the relationship between efficiency and band gap values or grain size were inversely proportional. This situation can be interpreted that as the grain sizes in the structure increase, the grain boundaries formed decrease, and the recombination rate of the charge carriers decreases. As a result, there is an increase in the efficiency to be obtained from the device. There are few studies in the literature reporting that the electrical properties of CZTS thin films are improved when the morphology and structural properties are improved [55,56].

3.4. Absorption behavior

The band-gap photon energy calculated values of the CZTS films were given in Table 1. The energy gap value of the CZTS compound, as a p-type direct band-gap semiconductor, is reported to be between 1.4 and 1.6 eV [57-59]. According to Table 1, it can be said that the estimated results are quite close to the optimum band gap for a solar cell.

Table 1. The IPCE and UV-Vis. results of un-doped and ETS doped CZTS samples.

Sample ID	S0	S1	S2	S3	S4	S5	S6
IPCE efficiencies (%)	5,44	3,42	10,63	6,72	8,55	7,88	6,02
E_g (eV)	1,49	1,44	1,37	1,42	1,45	1,46	1,47

The bandgap of a sample is greatly affected by its chemical composition, crystal structure, grain size and defects. The bandgap shows a strong dependence on the grain size at Figure 5. The bandgap decreased with increasing grain size. Table 1 summarizes the findings of this study [53].

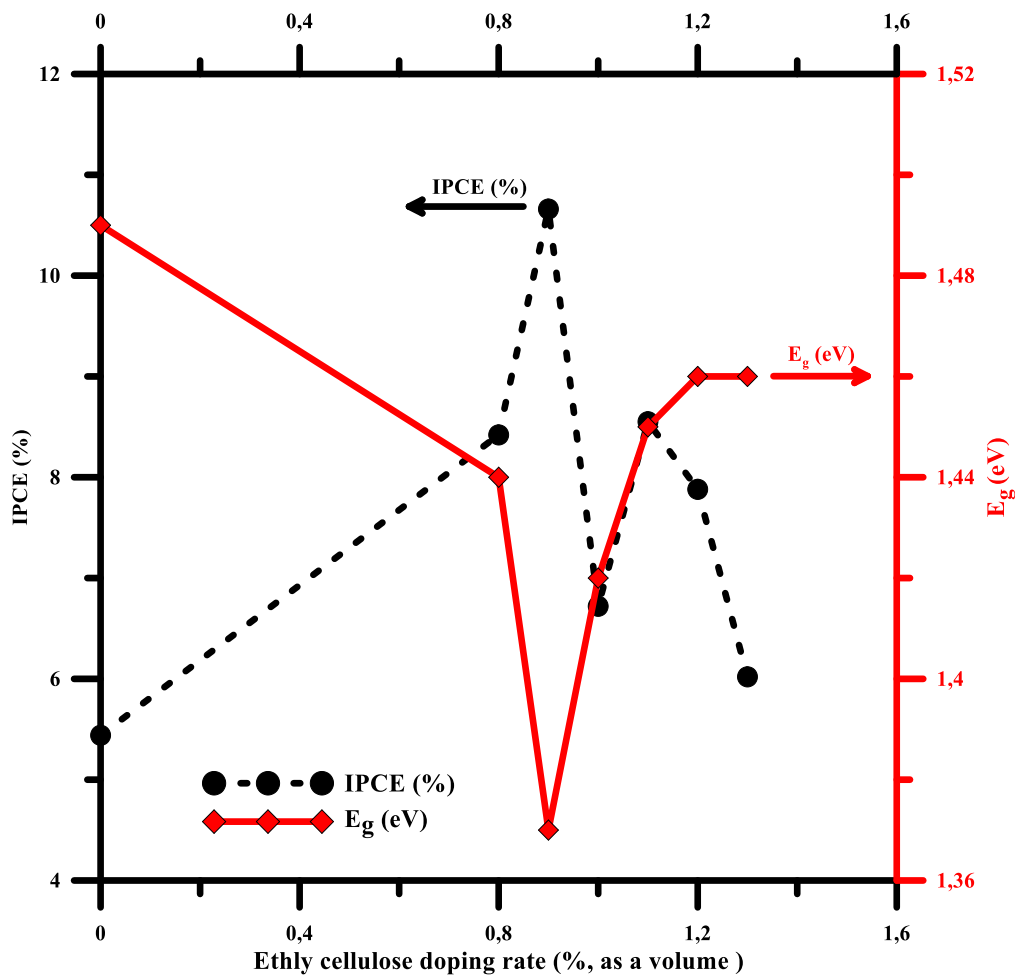


Figure 5. The doping ratio versus variation of the IPCE (%) and E_g (eV)

From Figure 5, as knowledge, additives used in aqueous methods control surface morphology, crystal structure, grain size, internal stress, corrosion behavior and even chemical composition [60]. As mentioned previously in SEM results, various amount of additive changed the morphology and structure of the films. As a result, variation

in the optical band gap values of the samples may attributed to changing of grain size, morphology, and chemical composition.

4. Conclusion

The samples prepared high-quality, dense CZTS thin films on Molybdenum coated SLG substrates by the sol-gel spin-coating method. The effects of the Ethyl cellulose temperature on the structural, morphological, compositional and optical properties of the films were investigated in detail.

- From the Raman spectroscopy results, no other phase's peaks were observed which suggests the absence of any binary and/or secondary phase which only the characteristic CZTS peaks were observed and confirmed the formation, phase purity and good crystalline quality of the CZTS films.
- From the FEG-SEM images, it can be interpreted that the surface roughness of the films decreases with increasing ethyl cellulose content. As can be seen that the named as S2 were observed a surface morphology consisting of large-grained structures with sizes ranging from approximately 1-2 μm .
- From the IPCE measurement result showed that S2 thin film was highest IPCE (%) efficiency value with 10,63% at 520 nm compared to IPCE (%) value of the pure one. According to the results, ETS additive plays an important role in the development of photovoltaic behavior of CZTS thin film.
- From the optical study results showed the optical band gap values were estimated to be between 1.37 and 1.49 eV depending on the ETS doping concentrations.

It was concluded that ETS can be suitable additive to get larger grains and higher efficiencies.

Funding

This research received no external funding.

Conflicts of interest

The authors declare no conflicts of interest.

References

1. Ojeda-Durán, E., Monfil-Leyva, K., Andrade-Arvizu, J., Becerril-Romero, I., Sánchez, Y., Fonoll-Rubio, R., ... & Saucedo, E. (2020). CZTS solar cells and the possibility of increasing VOC using evaporated Al_2O_3 at the CZTS/CdS interface. *Solar Energy*, 198, 696-703. <https://doi.org/10.1016/j.solener.2020.02.009>
2. Shockley, W. (1961). Problems related to pn junctions in silicon. *Solid-State Electronics*, 2(1), 35-60. [https://doi.org/10.1016/0038-1101\(61\)90054-5](https://doi.org/10.1016/0038-1101(61)90054-5)
3. Todorov, T. K., Reuter, K. B., & Mitzi, D. B. (2010). High-efficiency solar cell with earth-abundant liquid-processed absorber. *Advanced Materials*, 22(20), 156-159. <https://doi.org/10.1002/adma.200904155>
4. Nakazawa, K. I. (1988). Electrical and optical properties of stannite-type quaternary semiconductor thin films. *Japanese Journal of Applied Physics*, 27(11R), 2094-2097. <https://doi.org/10.1143/JJAP.27.2094>
5. Katagiri, H., Jimbo, K., Maw, W. S., Oishi, K., Yamazaki, M., Araki, H., & Takeuchi, A. (2009). Development of CZTS-based thin film solar cells. *Thin Solid Films*, 517(7), 2455-2460. <https://doi.org/10.1016/j.tsf.2008.11.002>
6. Mitzi, D. B., Gunawan, O., Todorov, T. K., Wang, K., & Guha, S. (2011). The path towards a high-performance solution-processed kesterite solar cell. *Solar Energy Materials and Solar Cells*, 95(6), 1421-1436. <https://doi.org/10.1016/j.solmat.2010.11.028>
7. Pawar, S. M., Pawar, B. S., Moholkar, A. V., Choi, D. S., Yun, J. H., Moon, J. H., ... & Kim, J. H. (2010). Single step electrosynthesis of $\text{Cu}_2\text{ZnSnS}_4$ (CZTS) thin films for solar cell application. *Electrochimica Acta*, 55(12), 4057-4061. <https://doi.org/10.1016/j.electacta.2010.02.051>
8. Sarswat, P. K., Snure, M., Free, M. L., & Tiwari, A. (2012). CZTS thin films on transparent conducting electrodes by electrochemical technique. *Thin Solid Films*, 520(6), 1694-1697. <https://doi.org/10.1016/j.tsf.2011.07.052>
9. Katagiri, H. (2005). $\text{Cu}_2\text{ZnSnS}_4$ thin film solar cells. *Thin Solid Films*, 480, 426-432. <https://doi.org/10.1016/j.tsf.2004.11.024>

10. Katagiri, H., Saitoh, K., Washio, T., Shinohara, H., Kurumadani, T., & Miyajima, S. (2001). Development of thin film solar cell based on $\text{Cu}_2\text{ZnSnS}_4$ thin films. *Solar Energy Materials and Solar Cells*, 65(1-4), 141-148. [https://doi.org/10.1016/S0927-0248\(00\)00088-X](https://doi.org/10.1016/S0927-0248(00)00088-X)
11. Wang, K., Gunawan, O., Todorov, T., Shin, B., Chey, S. J., Bojarczuk, N. A., ... & Guha, S. (2010). Thermally evaporated $\text{Cu}_2\text{ZnSnS}_4$ solar cells. *Applied Physics Letters*, 97(14), 143508. <https://doi.org/10.1063/1.3499284>
12. Fernandes, P. A., Salomé, P. M. P., & Da Cunha, A. F. (2011). Study of polycrystalline $\text{Cu}_2\text{ZnSnS}_4$ films by Raman scattering. *Journal of alloys and compounds*, 509(28), 7600-7606. <https://doi.org/10.1016/j.jallcom.2011.04.097>
13. Schubert, B. A., Marsen, B., Cinque, S., Unold, T., Klenk, R., Schorr, S., & Schock, H. W. (2011). $\text{Cu}_2\text{ZnSnS}_4$ thin film solar cells by fast coevaporation. *Progress in Photovoltaics: Research and Applications*, 19(1), 93-96. <https://doi.org/10.1002/pip.976>
14. Araki, H., Mikaduki, A., Kubo, Y., Sato, T., Jimbo, K., Maw, W. S., ... & Takeuchi, A. (2008). Preparation of $\text{Cu}_2\text{ZnSnS}_4$ thin films by sulfurization of stacked metallic layers. *Thin Solid Films*, 517(4), 1457-1460. <https://doi.org/10.1016/j.tsf.2008.09.058>
15. Seol, J. S., Lee, S. Y., Lee, J. C., Nam, H. D., & Kim, K. H. (2003). Electrical and optical properties of $\text{Cu}_2\text{ZnSnS}_4$ thin films prepared by rf magnetron sputtering process. *Solar energy materials and solar cells*, 75(1-2), 155-162. [https://doi.org/10.1016/S0927-0248\(02\)00127-7](https://doi.org/10.1016/S0927-0248(02)00127-7)
16. Yamaguchi, T., Kubo, T., Maeda, K., Niiyama, S., Imanishi, T., & Wakahara, A. (2009). Fabrication of $\text{Cu}_2\text{ZnSnS}_4$ thin films by sulfurization process from quaternary compound for photovoltaic device applications. In *Proceedings of the International Conference on Electrical Engineering* (pp. 1-4).
17. Fernandes, P. A., Salomé, P. M. P., Da Cunha, A. F., & Schubert, B. A. (2011). $\text{Cu}_2\text{ZnSnS}_4$ solar cells prepared with sulphurized dc-sputtered stacked metallic precursors. *Thin Solid Films*, 519(21), 7382-7385. <https://doi.org/10.1016/j.tsf.2010.12.035>
18. Fernandes, P. A., Salomé, P. M. P., & Da Cunha, A. F. (2009). Growth and Raman scattering characterization of $\text{Cu}_2\text{ZnSnS}_4$ thin films. *Thin Solid Films*, 517(7), 2519-2523. <https://doi.org/10.1016/j.tsf.2008.11.031>
19. Tanaka, K., Fukui, Y., Moritake, N., & Uchiki, H. (2011). Chemical composition dependence of morphological and optical properties of $\text{Cu}_2\text{ZnSnS}_4$ thin films deposited by sol-gel sulfurization and $\text{Cu}_2\text{ZnSnS}_4$ thin film solar cell efficiency. *Solar Energy Materials and Solar Cells*, 95(3), 838-842. <https://doi.org/10.1016/j.solmat.2010.10.031>
20. Tanaka, K., Oonuki, M., Moritake, N., & Uchiki, H. (2009). $\text{Cu}_2\text{ZnSnS}_4$ thin film solar cells prepared by non-vacuum processing. *Solar Energy Materials and Solar Cells*, 93(5), 583-587. <https://doi.org/10.1016/j.solmat.2008.12.009>
21. Maeda, K., Tanaka, K., Fukui, Y., & Uchiki, H. (2011). Influence of H_2S concentration on the properties of $\text{Cu}_2\text{ZnSnS}_4$ thin films and solar cells prepared by sol-gel sulfurization. *Solar Energy Materials and Solar Cells*, 95(10), 2855-2860. <https://doi.org/10.1016/j.solmat.2011.05.050>
22. Moritake, N., Fukui, Y., Oonuki, M., Tanaka, K., & Uchiki, H. (2009). Preparation of $\text{Cu}_2\text{ZnSnS}_4$ thin film solar cells under non-vacuum condition. *Physica Status Solidi c*, 6(5), 1233-1236. <https://doi.org/10.1002/pssc.200881158>
23. Sarswat, P. K., & Free, M. L. (2011). Demonstration of a sol-gel synthesized bifacial CZTS photoelectrochemical cell. *Physica Status Solidi (a)*, 208(12), 2861-2864. <https://doi.org/10.1002/pssa.201127216>
24. Fischereder, A., Rath, T., Haas, W., Amenitsch, H., Albering, J., Meischler, D., ... & Trimmel, G. (2010). Investigation of $\text{Cu}_2\text{ZnSnS}_4$ formation from metal salts and thioacetamide. *Chemistry of Materials*, 22(11), 3399-3406. <https://doi.org/10.1021/cm100058q>
25. Park, H., Hwang, Y. H., & Bae, B. S. (2013). Sol-gel processed $\text{Cu}_2\text{ZnSnS}_4$ thin films for a photovoltaic absorber layer without sulfurization. *Journal of sol-gel Science and Technology*, 65, 23-27. <https://doi.org/10.1007/s10971-012-2703-0>
26. Tanaka, K., Moritake, N., & Uchiki, H. (2007). Preparation of $\text{Cu}_2\text{ZnSnS}_4$ thin films by sulfurizing sol-gel deposited precursors. *Solar Energy Materials and Solar Cells*, 91(13), 1199-1201. <https://doi.org/10.1016/j.solmat.2007.04.012>
27. Yeh, M. Y., Lee, C. C., & Wu, D. S. (2009). Influences of synthesizing temperatures on the properties of $\text{Cu}_2\text{ZnSnS}_4$ prepared by sol-gel spin-coated deposition. *Journal of sol-gel Science and Technology*, 52, 65-68. <https://doi.org/10.1007/s10971-009-1997-z>
28. Chaudhuri, T. K., & Tiwari, D. (2012). Earth-abundant non-toxic $\text{Cu}_2\text{ZnSnS}_4$ thin films by direct liquid coating from metal-thiourea precursor solution. *Solar Energy Materials and Solar Cells*, 101, 46-50. <https://doi.org/10.1016/j.solmat.2012.02.012>
29. Yakuphanoglu, F. (2011). Nanostructure $\text{Cu}_2\text{ZnSnS}_4$ thin film prepared by sol-gel for optoelectronic applications. *Solar Energy*, 85(10), 2518-2523. <https://doi.org/10.1016/j.solener.2011.07.012>
30. Sarswat, P. K., & Free, M. L. (2012). An evaluation of depletion layer photoactivity in $\text{Cu}_2\text{ZnSnS}_4$ thin film. *Thin Solid Films*, 520(13), 4422-4426. <https://doi.org/10.1016/j.tsf.2012.02.066>

31. Zhang, X., Shi, X., Ye, W., Ma, C., & Wang, C. (2009). Electrochemical deposition of quaternary $\text{Cu}_2\text{ZnSnS}_4$ thin films as potential solar cell material. *Applied Physics A*, 94, 381-386. <https://doi.org/10.1007/s00339-008-4815-5>
32. Scragg, J. J., Berg, D. M., & Dale, P. J. (2010). A 3.2% efficient Kesterite device from electrodeposited stacked elemental layers. *Journal of Electroanalytical Chemistry*, 646(1-2), 52-59. <https://doi.org/10.1016/j.jelechem.2010.01.008>
33. Scragg, J. J., Dale, P. J., & Peter, L. M. (2008). Towards sustainable materials for solar energy conversion: Preparation and photoelectrochemical characterization of $\text{Cu}_2\text{ZnSnS}_4$. *Electrochemistry Communications*, 10(4), 639-642. <https://doi.org/10.1016/j.elecom.2008.02.008>
34. Mali, S. S., Patil, B. M., Betty, C. A., Bhosale, P. N., Oh, Y. W., Jadkar, S. R., ... & Patil, P. S. (2012). Novel synthesis of kesterite $\text{Cu}_2\text{ZnSnS}_4$ nanoflakes by successive ionic layer adsorption and reaction technique: characterization and application. *Electrochimica Acta*, 66, 216-221. <https://doi.org/10.1016/j.electacta.2012.01.079>
35. Mali, S. S., Shinde, P. S., Betty, C. A., Bhosale, P. N., Oh, Y. W., & Patil, P. S. (2012). Synthesis and characterization of $\text{Cu}_2\text{ZnSnS}_4$ thin films by SILAR method. *Journal of physics and chemistry of solids*, 73(6), 735-740. <https://doi.org/10.1016/j.jpics.2012.01.008>
36. Su, Z., Yan, C., Sun, K., Han, Z., Liu, F., Liu, J., ... & Liu, Y. (2012). Preparation of $\text{Cu}_2\text{ZnSnS}_4$ thin films by sulfurizing stacked precursor thin films via successive ionic layer adsorption and reaction method. *Applied Surface Science*, 258(19), 7678-7682. <https://doi.org/10.1016/j.apsusc.2012.04.120>
37. Shin, S. W., Pawar, S. M., Park, C. Y., Yun, J. H., Moon, J. H., Kim, J. H., & Lee, J. Y. (2011). Studies on $\text{Cu}_2\text{ZnSnS}_4$ (CZTS) absorber layer using different stacking orders in precursor thin films. *Solar energy materials and solar cells*, 95(12), 3202-3206. <https://doi.org/10.1016/j.solmat.2011.07.005>
38. Prabhakar, T., & Jampana, N. (2011). Effect of sodium diffusion on the structural and electrical properties of $\text{Cu}_2\text{ZnSnS}_4$ thin films. *Solar Energy Materials and Solar Cells*, 95(3), 1001-1004. <https://doi.org/10.1016/j.solmat.2010.12.012>
39. Rajamathi, M., & Seshadri, R. (2002). Oxide and chalcogenide nanoparticles from hydrothermal/solvothermal reactions. *Current Opinion in Solid State and Materials Science*, 6(4), 337-345. [https://doi.org/10.1016/S1359-0286\(02\)00029-3](https://doi.org/10.1016/S1359-0286(02)00029-3)
40. Peters, I. M., Gallegos, C. D. R., Sofia, S. E., & Buonassisi, T. (2019). The value of efficiency in photovoltaics. *Joule*, 3(11), 2732-2747.
41. Lee, K. M., Suryanarayanan, V., & Ho, K. C. (2006). The influence of surface morphology of TiO_2 coating on the performance of dye-sensitized solar cells. *Solar Energy Materials and Solar Cells*, 90(15), 2398-2404. <https://doi.org/10.1016/j.solmat.2006.03.034>
42. Muniz, E. C., Góes, M. S., Silva, J. J., Varela, J. A., Joanni, E., Parra, R., & Bueno, P. R. (2011). Synthesis and characterization of mesoporous TiO_2 nanostructured films prepared by a modified sol-gel method for application in dye solar cells. *Ceramics International*, 37(3), 1017-1024. <https://doi.org/10.1016/j.ceramint.2010.11.014>
43. Maldonado-Valdivia, A. I., Galindo, E. G., Ariza, M. J., & Garcia-Salinas, M. J. (2013). Surfactant influence in the performance of titanium dioxide photoelectrodes for dye-sensitized solar cells. *Solar Energy*, 91, 263-272. <https://doi.org/10.1016/j.solener.2013.02.009>
44. Xu, S., Zhou, C. H., Yang, Y., Hu, H., Sebo, B., Chen, B. L., ... & Zhao, X. (2011). Effects of ethanol on optimizing porous films of dye-sensitized solar cells. *Energy & Fuels*, 25(3), 1168-1172. <https://doi.org/10.1021/ef101546a>
45. Kahraman, S., Çetinkaya, S., Podlogar, M., Bernik, S., Çetinkara, H. A., & Güder, H. S. (2013). Effects of the sulfurization temperature on sol gel-processed $\text{Cu}_2\text{ZnSnS}_4$ thin films. *Ceramics International*, 39(8), 9285-9292. <https://doi.org/10.1016/j.ceramint.2013.05.039>
46. Ghos, B. C., Farhad, S. F. U., Patwary, M. A. M., Majumder, S., Hossain, M. A., Tanvir, N. I., ... & Guo, Q. (2021). Influence of the substrate, process conditions, and postannealing temperature on the properties of ZnO thin films grown by the successive ionic layer adsorption and reaction method. *ACS omega*, 6(4), 2665-2674. <https://doi.org/10.1021/acsomega.0c04837>
47. Kitahara, K., Ishii, T., Suzuki, J., Bessyo, T., & Watanabe, N. (2011). Characterization of defects and stress in polycrystalline silicon thin films on glass substrates by Raman microscopy. *International Journal of Spectroscopy*, 2011, 632139. <https://doi.org/10.1155/2011/632139>
48. Choi, H. C., Jung, Y. M., & Kim, S. B. (2005). Size effects in the Raman spectra of TiO_2 nanoparticles. *Vibrational spectroscopy*, 37(1), 33-38. <https://doi.org/10.1016/j.vibspec.2004.05.006>
49. Rajalakshmi, M., Arora, A. K., Bendre, B. S., & Mahamuni, S. (2000). Optical phonon confinement in zinc oxide nanoparticles. *Journal of Applied Physics*, 87(5), 2445-2448. <https://doi.org/10.1063/1.372199>
50. Yang, C. L., Wang, J. N., Ge, W. K., Guo, L., Yang, S. H., & Shen, D. Z. (2001). Enhanced ultraviolet emission and optical properties in polyvinyl pyrrolidone surface modified ZnO quantum dots. *Journal of Applied Physics*, 90(9), 4489-4493. <https://doi.org/10.1063/1.1406973>

51. Guo, L., Yang, S., Yang, C., Yu, P., Wang, J., Ge, W., & Wong, G. K. (2000). Highly monodisperse polymer-capped ZnO nanoparticles: Preparation and optical properties. *Applied physics letters*, 76(20), 2901-2903. <https://doi.org/10.1063/1.126511>
52. Alim, K. A., Fonoberov, V. A., & Balandin, A. A. (2005). Origin of the optical phonon frequency shifts in ZnO quantum dots. *Applied Physics Letters*, 86(5), 053103. <https://doi.org/10.1063/1.1861509>
53. Jain, P., & Arun, P. (2013). Influence of grain size on the band-gap of annealed SnS thin films. *Thin Solid Films*, 548, 241-246. <https://doi.org/10.1016/j.tsf.2013.09.089>
54. Ansari, M. Z., & Khare, N. (2014). Structural and optical properties of CZTS thin films deposited by ultrasonically assisted chemical vapour deposition. *Journal of Physics D: Applied Physics*, 47(18), 185101. <https://doi.org/10.1088/0022-3727/47/18/185101>
55. Wang, H. H., Su, C., Wu, C. Y., Tsai, H. B., & Li, W. R. (2014). The effect of ethyl cellulose on TiO₂ pastes for DSSCs application. *International Journal of Nanotechnology*, 11(12), 1138-1147. <https://doi.org/10.1504/IJNT.2014.065140>
56. Li, H., Xie, Z., Zhang, Y., & Wang, J. (2010). The effects of ethyl cellulose on PV performance of DSSC made of nanostructured ZnO pastes. *Thin Solid Films*, 518(24), e68-e71. <https://doi.org/10.1016/j.tsf.2010.03.125>
57. Delbos, S. (2012). Kesterite thin films for photovoltaics: a review. *EPJ Photovoltaics*, 3, 35004. <https://doi.org/10.1051/epjpv/2012008>
58. Kahraman, S., Çetinkaya, S., Podlogar, M., Bernik, S., Çetinkara, H. A., & Güder, H. S. (2013). Effects of the sulfurization temperature on sol gel-processed Cu₂ZnSnS₄ thin films. *Ceramics International*, 39(8), 9285-9292. <https://doi.org/10.1016/j.ceramint.2013.05.039>
59. Kahraman, S., Çakmak, H. M., Çetinkaya, S., Çetinkara, H. A., & Güder, H. S. (2013). The effects of coumarin additive on the properties of ZnO nanostructures. *Journal of Physics and Chemistry of Solids*, 74(4), 565-569. <https://doi.org/10.1016/j.jpics.2012.12.005>
60. Maniam, K. K., & Paul, S. (2021). Corrosion performance of electrodeposited zinc and zinc-alloy coatings in marine environment. *Corrosion and Materials Degradation*, 2(2), 163-189. <https://doi.org/10.3390/cmd2020010>



© Author(s) 2023. This work is distributed under <https://creativecommons.org/licenses/by-sa/4.0/>